CHEMICAL ENGINEERING TRANSACTIONS
VOL. 76, 2019
A publication of AIDIC
The Italian Association of Chemical Engineering
Online at www.aidic.it/cet
Guest Editors: Petar S. Varbanov, Timothy G. Walmsley, Jiří J. Klemeš, Panos Seferlis

ISBN 978-88-95608-73-0; **ISSN** 2283-9216
DOI: 10.3303/CET1976027

Nonlinear Finite Element Analysis-Based Flow Distribution Model for Engineering Practice

Tomáš Létal*, Vojtěch Turek, Dominika Fialová

Institute of Process Engineering, Faculty of Mechanical Engineering, Brno University of Technology, Technická 2, 61600 Brno, Czech Republic
letal@fme.vutbr.cz

In engineering practice, it is common that heat transfer equipment containing tube bundles are designed under the assumption of uniform flow distribution. Such a flawed approach may easily lead to various operating problems (increased local fouling rates, mechanical failures, etc.) and significantly shortened service life. Accordingly, knowing the flow pattern in the bundle is crucial to proper design of the respective apparatuses. Although computational fluid dynamics (CFD) models yield very accurate data, due to their inherent computational cost they are not really suitable for evaluation of large sets of possible flow system geometries. Algebraic or otherwise greatly simplified models, on the other hand, are acceptable in terms of computational performance, but generally suffer from low accuracy and limited applicability to more complex meshes. This paper therefore proposes a computationally efficient flow distribution model whose principle is analogous to nonlinear finite element analysis (FEA). Unlike in many other simplified models, no special correction algorithms or user modifications are needed here because the underlying system of equations is solved in the matrix form and the corrector step is mesh-independent. Additionally, results provided by the model are compared to the data obtained using detailed CFD analyses of several different flow systems. Although the accuracy of the model does not match that of CFD, it can still be used at the beginning of a design process to discard the obviously unsuitable options, which would otherwise have to be evaluated via lengthy CFD simulations.

1. Introduction

Knowledge of the final fluid flow distribution among individual channels of a parallel flow system is crucial in many engineering fields. Although this information is useful primarily in the design stage, it can also provide answers in case of troubleshooting. Flow distribution data are used to assess performance and reliability of heat exchangers (in terms of fouling propensity or the resulting thermal and mechanical loading of the tube bundle), product quality (e.g. when a hydrocarbon fuel is cracked in a heated parallel flow system), etc. The most common approach to this problem nowadays is numerical investigation via standard CFD models. A multitude of such studies are therefore available ranging from those focusing on various header (Jiang et al., 2018a) or parallel flow channel (Jiang et al., 2018b) shapes, shell-and-tube (Labbadlia et al., 2017) or compact (Zhou et at., 2017) heat exchangers, microchannel (Wei et al., 2016) or fuel cell (Zhao et al., 2017) applications, solar thermal collectors (Wei et al., 2017), separation equipment (Chang et al., 2019), and other areas all the way to e.g. datacentre cooling (Yue et al., 2019). The results obtained this way are very accurate, but there is a significant cost in terms of computational complexity. Other factors that must be considered are the creation of the necessary mesh of sufficient quality and often a rather non-trivial setup of the CFD model itself. In other words, these models are suitable if a few apparatuses are to be analysed, but not in cases when a large batch of different geometries must be evaluated (e.g. when shape optimisation is to be carried out).
Modelling approaches based on CFD, or somewhat simplified CFD, can also be encountered. These are often employed to simulate less complex flow systems or when certain phenomena are less important from the modelling point of view and can thus be neglected. Here the range of studies is also very wide and includes e.g. inter-plate flow in plate heat exchangers (Yoon and Jeong, 2017), bifurcating distribution channels (Cao et al., 2018), or even ways to improve the numerical performance of the models themselves (Turek, 2018). The respective simulations, however, are still quite time-consuming with the necessary mesh creation being a

Paper Received: 11/03/2019; Revised: 27/03/2019; Accepted: 28/03/2019
Please cite this article as: Letal T., Turek V., Fialova D., 2019, Nonlinear Finite Element Analysis-Based Flow Distribution Model for Engineering Practice, Chemical Engineering Transactions, 76, 157-162 DOI:10.3303/CET1976027

relatively complex task as well. Such models are not really suitable in spite of their being partially simplified in comparison to the standard CFD ones.
The simplest flow models, on the other hand, usually employ a wire mesh instead of a fully-3D mesh and are often analytical in nature, thus also very fast. Their accuracy may suffer due to the many simplifications that are implemented, yet they are used in many engineering areas because of their efficiency and ease of automation. The most common applications include heating, ventilation, and air conditioning (HVAC) (Ye, 2017) and flow distribution systems with generally very limited numbers of rows of parallel channels (Hao et al., 2016). One can encounter even models for non-standard conditions such as supercritical flow (Liu et al., 2018). The inherent property of the models in question is that nonlinearities are included directly, which prohibits usage of matrix solvers and hence makes efficient evaluation of larger meshes very problematic.
The best research area to draw parallels from therefore seems to be water distribution networks, which, due to the sizes of such networks, necessitates matrix implementation. Here, however, the models are focused in a largely different direction. They consider simple network flow (with the network structure often being the sought result) and try to meet the specified local water demands (or aim to localise leakages, model the spreading of contaminants, etc.). In other words, these commonly work with just the network edge capacities instead of being concerned with the hydraulics-related phenomena. In rare cases though (see e.g. Dudar and Dudar, 2017), the fluid distribution network problem is approached from the perspective of finite element analysis (FEA) and such models then attempt to properly include also the pressure losses etc. The aim of the present study is to extend this modelling strategy to process and power equipment (e.g. heat exchangers) where the built-in flow systems are often much too complex for the simple flow models to be used.

2. Mathematical model

The model is based on Hooke's law applied to fluid flow in a channel, that is, mass flow rate is linearly dependent on the product of "compliance" of the respective channel (it being a function of hydraulic resistance) and pressure drop therein. Just as in case of many other simplified models, the effect of turbulence is not included. The basic equation governing the flow of a fluid with constant physical properties through a channel then is

$$\dot{m} = k\Delta p \tag{1}$$

in which $\dot{m}$ denotes mass flow rate, k compliance, and Δp pressure drop. The actual value of k for a given channel can be estimated from Eq(1) using the Darcy-Weisbach equation for Δp (White, 1998),

$$\Delta p = 0.5 f l d_{\mathrm{h}}^{-1} \rho v^2 \tag{2}$$

where f denotes the Darcy friction factor, l length of the channel, d_{h} its hydraulic diameter, ρ density of the fluid, and v its mean flow velocity. Channel cross-sectional area and other characteristics, which are necessary to estimate f, are calculated from the corresponding mesh properties.

2.1 Structure and mathematical representation of the quasi-3D mesh

The mesh consists of nodes which are interconnected either by straight, directed edges representing virtual flow channels, or T-shaped elements ("T-joints", a special set of at least three straight edges – see further) in which the flow is divided or combined. Straight edges, as well as the straight portions of a T-shaped element, are assumed to have constant cross-sections and are uniquely identifiable by the respective boundary nodes. For an arbitrary mesh, the following additional assumptions are made:

- The pressure gradient over the edge is given by the difference in total pressures in its boundary nodes.
- Physical properties of the fluid are constant within one iteration and are obtained using the mean edge pressure and the corresponding enthalpy (or temperature).

The general set of equations that must hold for an arbitrary edge can then be written as

$$\mathbf{K}_{ij}\mathbf{p}_{ij} = \dot{\mathbf{m}}_{ij}, \quad \text{with} \quad \mathbf{K}_{ij} = \begin{bmatrix} k_{ii} & k_{ij} \\ k_{ji} & k_{jj} \end{bmatrix}, \ \mathbf{p}_{ij} = \begin{bmatrix} p_i \\ p_j \end{bmatrix}, \ \text{and} \ \dot{\mathbf{m}}_{ij} = \begin{bmatrix} \dot{m}_i \\ \dot{m}_j \end{bmatrix} \tag{3}$$

in which $\mathbf{K}_{ij}$ denotes the compliance matrix of the directed edge connecting the nodes i and j, $\mathbf{p}_{ij}$ the respective vector holding pressures in the boundary nodes, and $\dot{\mathbf{m}}_{ij}$ the vector of mass flow rates in these nodes. It can be shown that the compliance matrix generally attains the following form:

$$\mathbf{K}_{ij} = \begin{bmatrix} k_{ij} & -k_{ij} \\ -k_{ij} & k_{ij} \end{bmatrix}, \text{ where } \quad k_{ij} = \frac{2\rho_{ij} A_{ij} d_{\mathrm{h},ij}^2}{C_{ij}\mu_{ij} l_{ij}} \tag{4}$$

In the equation above, A_{ij} is the cross-sectional area of the respective edge, C_{ij} the constant from the formula for calculation of laminar friction factor, and μ_{ij} the dynamic viscosity of the fluid. Should an external acceleration

field be in effect (e.g. due to gravity), also the hydrostatic pressure head must be included via $p_{\mathrm{h},ij} = \rho_{ij}(\mathbf{a}_{ij} \cdot \mathbf{l}_{ij})$, in which $\mathbf{a}_{ij}$ and $\mathbf{l}_{ij}$ denote the external acceleration vector and the vector representing the directed edge, respectively. This yields a new set of equations replacing Eq(3),

$$\begin{bmatrix} k_{ij} & -k_{ij} \\ -k_{ij} & k_{ij} \end{bmatrix} \begin{bmatrix} p_i - p_{\mathrm{h},ij} \\ p_j \end{bmatrix} = \begin{bmatrix} \dot{m}_i \\ \dot{m}_j \end{bmatrix} \quad \text{or} \quad \mathbf{K}_{ij}\mathbf{p}_{ij} = \dot{\mathbf{m}}_{ij} + \dot{\mathbf{m}}_{\mathrm{h},ij} \tag{5}$$

where $\dot{\mathbf{m}}_{\mathrm{h},ij}$ is the mass flow rate correction vector accounting for the effect of the external acceleration field.
In case of a set of interconnected edges, there must be at least one source node and at least one (different) sink node. In other words, while in the majority of nodes the sums of mass flow rates must be zero, in the sources and sinks these attain non-zero values. The solution is then computed iteratively. At the beginning of this process, the complete set of equations is constructed from Eq(5) for all the edges in the set with the elements in the compliance matrix and the right-hand side (RHS) vector being obtained from the boundary conditions and the initial estimate. In the next step (i.e., the predictor step), the set of equations is solved, yielding a new estimate of the pressure vector. This vector corresponds to the system of equations not including any nonlinearities, which are considered in the subsequent corrector step (see Sections 2.2 and 2.3). Lastly, the elements in the compliance matrix and the RHS vector are updated, and a new predictor step is carried out. Dudar and Dudar (2017) suggest that the next-iteration (I + 1) value of k_{ij} should be calculated using $k_{ij,I+1} = k_{ij,I}(\dot{m}_{ij,I,\mathrm{corr}}/\dot{m}_{ij,I,\mathrm{lin}})$, where $\dot{m}_{ij,I,\mathrm{corr}}$ denotes the corrected mass flow rate including the effect of nonlinearities (i.e., from the corrector step) and $\dot{m}_{ij,I,\mathrm{lin}}$ the linear estimate from the predictor step. This results in relatively poor convergence behaviour and requires additional relaxation. In the present study, the elements of the compliance matrix are therefore updated using the square root of the mass flow ratio as indicated in Figure 1. Although this approach results in longer computational times, convergence is much smoother, and no additional relaxation is needed.

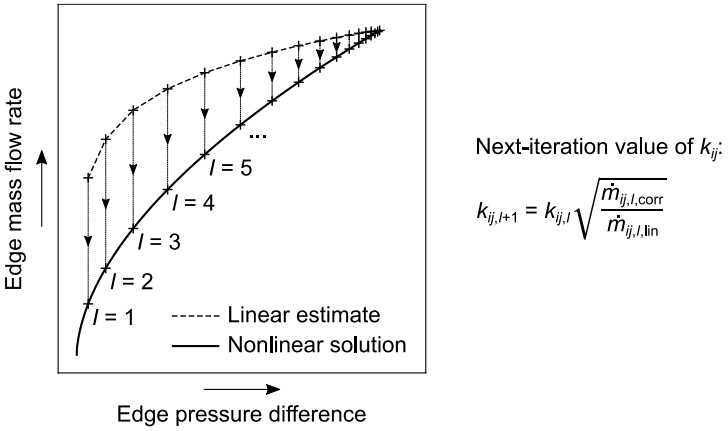

Figure 1: Typical convergence history of the mass flow rate through an edge connecting nodes i and j with the next-iteration (I + 1) value of k_{ij} being obtained using the square root of the ratio of the current corrected (nonlinear) and estimated (linear) flow rates

2.2 Including typical nonlinearities

Nonlinearities are introduced into the model for example by frictional pressure drop, minor losses, or the dependence of fluid properties on pressure (because pressure is unknown during the solution process). The most basic scenario, which will be discussed first, is flow through a straight edge where pressure changes only due to friction. This is for an arbitrary edge given by the Darcy-Weisbach equation in which the Darcy friction factor can be estimated e.g. using the Churchill approximation (Churchill, 1977). The resulting nonlinear dependence of mass flow rate on edge pressure difference is shown as the thick solid line in Figure 2. Because the pressure difference estimates are known from the predictor step and the fact that the respective dependence is monotonous, in the corrector step one can use e.g. the bisection method to quickly get the corresponding nonlinear solution, $\dot{m}_{ij,\mathrm{corr}}$. Zero mass flow rate can then be taken as one of the bounds for the bisection method while the other bound can be easily estimated using the first-order Taylor approximation (i.e., the tangent) at $\Delta p_{ij} = 0$. Should other common nonlinearities be included as well, the nonlinear solution curve would be different, but still monotonous. The same procedure to obtain $\dot{m}_{ij,\mathrm{corr}}$ would therefore be applicable.

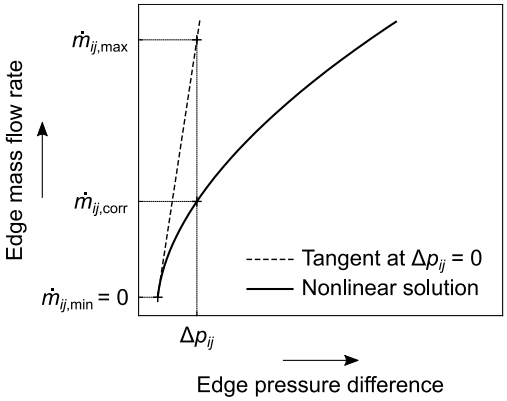

Figure 2: Estimation of bounds for the bisection method used in the corrector step for an edge connecting nodes i and j, for which the corresponding pressure difference is Δp_{ij}

2.3 T-joints

Nonlinearities are also introduced in T-joints where the fluid is split into or merged from multiple separate streams. Each T-joint comprises three or more T-connected mesh edges. Two edges represent the main channel (distributor or collector) and the remaining edges the attached branches. For modelling purposes, the main channel edges are directed towards the branch (i.e., edge flow velocity is positive if the fluid flows towards the virtual shared node) while the branch edges are directed out of the T-joint. Frictional pressure drop is dealt with just as in case of the regular (straight) edges. Minor losses are included via minor loss coefficients taken from relevant literature. The static pressure changed due to the flow being split or merged is obtained in the manner suggested by Bailey (1975).

Having a T-joint consisting of edges *ij*, *kj*, and *jl*, where the edges *ij* and *kj* form the main channel and the edge *jl* represents the branch (see the schematic in Figure 3), one can calculate the cross-sectional area ratio $R_A = A_{jl} / A_{ij} = A_{jl} / A_{kj}$ (it is assumed that $A_{ij} = A_{kj}$). Then it can be shown that the velocity ratio

$$R_v = |v_{jl}| \,/\, \max\{|v_{ij}|, |v_{kj}|\} \in [0, 2/R_A], \tag{6}$$

where v_{ij}, v_{kj}, and v_{jl} are the flow velocities in the main channel edges and the branch edge, respectively. The interval mentioned in Eq(6) also is the one to which the bisection method is applied to get the final value of R_v and thus the final edge velocities. Because the corresponding boundary node pressures (p_i, p_k, and p_l) are known from the predictor step, one can take as the initial estimate of v_{jl} for instance the value obtained from the minor loss equation with the pressure drop calculated from p_k and p_l. Eq(6) then yields for the current estimate of R_v from the bisection method the velocities v_{ij} and v_{kj} (these are interdependent because of the law of conservation of mass). Now all the velocity estimates are known and are used to check whether the main channel pressure difference, including the static pressure regain, is close enough to the one given by the known node pressures, p_i and p_k. If not, the range of the bisection method is halved accordingly, and the entire process is repeated. Example convergence history for the corrector step is shown in Figure 3.

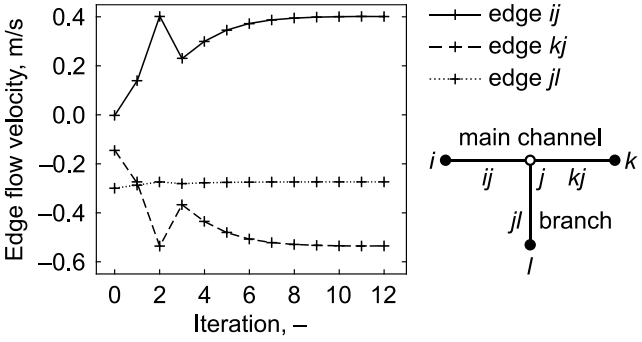

Figure 3: Typical convergence history for the corrector step carried out for a T-joint with boundary nodes i, k, and l; in this example, the flows are merged in the main channel while the respective flow direction is $i \rightarrow k$

2.4 Boundary conditions

In each inlet and outlet node, either the mass flow rate or the pressure must be prescribed. Every mesh edge is assumed to be a closed channel with walls featuring a specified absolute roughness, which is then utilised for the estimation of Darcy friction factors. As of now, the system is assumed to be adiabatic. However, future enhancement of the model by adding heat transfer capability to the straight mesh elements is planned so that e.g. heat transfer through tube walls can be simulated.

3. Model validation

The model has been implemented using the NumPy scientific computing package (Oliphant, 2006). Several different flow systems similar to cross-flow tube bundles common e.g. in air coolers were evaluated (see Table 1). Both the U and Z flow arrangements were considered. The systems were adiabatic with cuboid headers and water at 300 K being used as the process medium. The obtained flow distributions within the bundles (i.e., individual tube mass flow rates) were then compared with data yielded by detailed CFD simulations. Relative tube mass flow rate errors calculated as $100(\dot{m}/\dot{m}_{\mathrm{CFD}} - 1)$ were always below 4 %. An example plot of these errors for a subset of the flow systems and a plot of the actual mass flow rates for one of them are shown in Figure 4. In terms of performance, all test runs finished in at most tens of seconds.

Table 1: Evaluated flow systems; all tubes were with inner diameters of 10 mm and lengths of 2,000 mm

Flow system	Headers (W × H × L)	Mass flow rate	Tube bundle
A	40 × 40 × 320 mm	6.4 kg/s	2 rows with 20 tubes each, 90°
B	40 × 40 × 280 mm	9.6 kg/s	3 rows with 10 tubes each, 60°
C	55 × 55 × 320 mm	19.2 kg/s	3 rows with 20 tubes each, 90°
D	55 × 55 × 280 mm	16.0 kg/s	5 rows with 10 tubes each, 60°
E	65 × 70 × 235 mm	16.0 kg/s	5 rows with 10 tubes each, 45°
F	70 × 70 × 320 mm	25.6 kg/s	4 rows with 20 tubes each, 90°

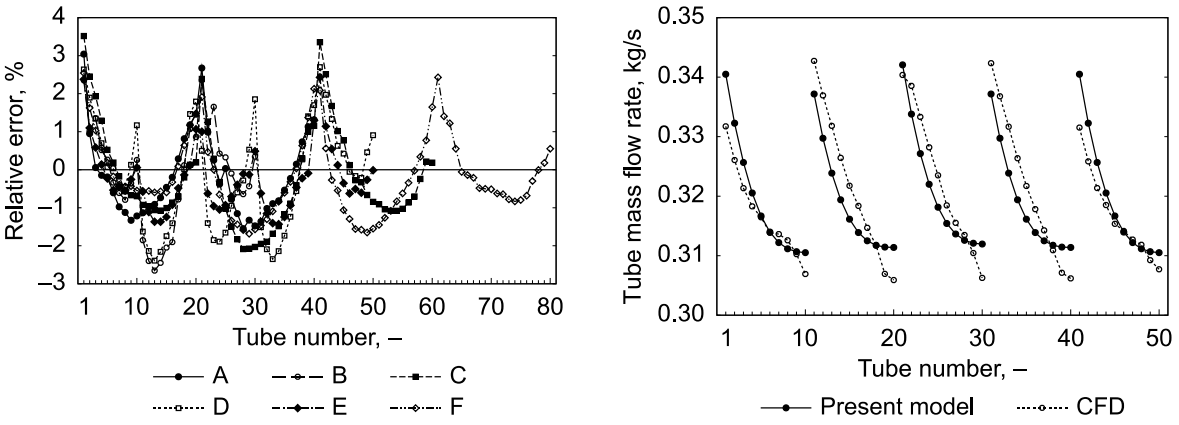

(a) relative errors (b) tube mass flow rates for flow system D

Figure 4: Tube mass flow rate relative errors with respect to the data from detailed CFD simulations of the U-arranged flow systems from Table 1 (a) and the comparison of mass flow rates through individual tubes of the U-arranged flow system D from Table 1

4. Conclusions

The model discussed in this paper represents a robust way to estimate flow distribution in a system consisting of a large set of parallel flow channels. The downsides of the present model are its being steady-state and adiabatic; however, implementation of the respective enhancements is planned for the near future.

The preliminary tests carried out using the developed computer code yielded flow distribution data with relative errors – compared to the results from detailed CFD simulations – of less than 4 %. The mass flow rate trends per individual tube rows in the bundles were not identical to those obtained using CFD, but the differences were still acceptable given the intended purpose of the model. As for its numerical performance, the time needed to evaluate a single flow system configuration never exceeded 30 s, whereas the corresponding detailed CFD simulations required units of hours to finish when run in parallel on 16 or more CPU cores.

In spite of the present model not being as accurate as CFD, its ultimate benefit lies in the fact that it can be easily automated. Process engineers can therefore use it to effortlessly estimate flow distribution in many different geometries, and then use CFD to evaluate in detail only the promising ones. In other words, the developed computer code can be considered a “pre-screening sieve” with which process engineers can save themselves significant amounts of time and effort.

Acknowledgments

This research has been supported by the project No. CZ.02.1.01/0.0/0.0/16_026/0008413 “Strategic partnership for environmental technologies and energy production”, which has been co-funded by the Czech Ministry of Education, Youth and Sports within the EU Operational Programme Research, Development and Education.

References

Bailey B., 1975, Fluid flow in perforated pipes, Journal of Mechanical Engineering Science, 17, 338–347.

Cao J., Kraut M., Dittmeyer R., Zhang L., Xu H., 2018, Numerical analysis on the effect of bifurcation angle and inlet velocity on the distribution uniformity performance of consecutive bifurcating fluid flow distributors, International Communications in Heat and Mass Transfer, 93, 60–65.

Chang Y., Wang H., Jin J., Liu Z., Lv W., 2019, Flow distribution and pressure drop in UZ-type mini-hydrocyclone group arranged in compact parallel manifolds, Experimental Thermal and Fluid Science, 100, 114–123.

Churchill S., 1977, Friction-factor equation spans all fluid and flow regimes, Chemical Engineering, 84, 91–92.

Dudar O.I., Dudar E.S., 2017, Application of 1 D finite element method in combination with laminar solution method for pipe network analysis, In: IOP Conference Series: Materials Science and Engineering, Vol 262, paper ID 012085.

Hao Y., Wang Y., Hu T., 2016, The flow distribution in the parallel tubes of the cavity receiver under variable heat flux, Applied Thermal Engineering, 108, 641–649.

Jiang Y., Qin J., Xu Y., Zhang S., Chetehouna K., Gascoin N., Bao W., 2018a, The influences of the header geometry on hydrocarbon fuel flow distribution in compact parallel channels, Aerospace Science and Technology, 79, 318–327.

Jiang Y., Xu Y., Qin J., Zhang S., Chetehouna K., Gascoin N., Bao W., 2018b, The flow rate distribution of hydrocarbon fuel in parallel channels with different cross section shapes, Applied Thermal Engineering, 137, 173–183.

Labbadlia O., Laribi B., Chetti B., Hendrick P., 2017, Numerical study of the influence of tube arrangement on the flow distribution in the header of shell and tube heat exchangers, Applied Thermal Engineering, 126, 315–321.

Liu J., Li H., Lei X., Zhang Q., Li L., 2018, An improved model on flow distributions of supercritical pressure water in parallel heated pipes, Applied Thermal Engineering, 130, 793–803.

Oliphant T.E, 2006, A guide to NumPy, Trelgol Publishing, Spanish Fork, UT, USA.

Turek V., 2018, On improving computational efficiency of simplified fluid flow models, Chemical Engineering Transactions, 70, 1447–1452.

Wei M., Boutin G., Fan Y., Luo L., 2016, Numerical and experimental investigation on the realization of target flow distribution among parallel mini-channels, Chemical Engineering Research and Design, 113, 74–84.

Wei M., Fan Y., Luo L., Flamant G., 2017, Design and optimization of baffled fluid distributor for realizing target flow distribution in a tubular solar receiver, Energy, Renewable Energy and Energy Storage Systems, 136, 126–134.

White F., 1998, Fluid Mechanics, 4th ed., McGraw-Hill Inc., New York, NY, USA.

Ye W.-B., 2017, Design method and modeling verification for the uniform air flow distribution in the duct ventilation, Applied Thermal Engineering, 110, 573–583.

Yoon W., Jeong J.H., 2017, Development of a numerical analysis model using a flow network for a plate heat exchanger with consideration of the flow distribution, International Journal of Heat and Mass Transfer, 112, 1–17.

Yue C., Zhang Q., Zhai Z., Ling L., 2019, Numerical investigation on thermal characteristics and flow distribution of a parallel micro-channel separate heat pipe in data center, International Journal of Refrigeration, 98, 150–160.

Zhao C., Yang J., Zhang T., Yan D., Pu J., Chi B., Li J., 2017, Numerical simulation of flow distribution for external manifold design in solid oxide fuel cell stack, International Journal of Hydrogen Energy, 42, 7003–7013.

Zhou J., Sun Z., Ding M., Bian H., Zhang N., Meng Z., 2017, CFD simulation for flow distribution in manifolds of central-type compact parallel flow heat exchangers, Applied Thermal Engineering, 126, 670–677.